Plant Stress 11 (2024) 100336

Contents lists available at ScienceDirect

Plant Stress

journal homepage: www.sciencedirect.com/journal/plant-stress

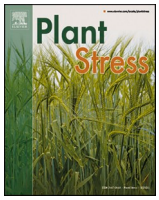

Low nitrogen status affects isoflavonoid production and flavonol decoration in *Lotus corniculatus*

Kristina Trush [a], Martina Gavurová [a], María Dolores Monje-Rueda [b], Vladislav Kolarčik [a], Michaela Bačovčinová [a], Marco Betti [b], Peter Paľove-Balang [a,*]

[a] Institute of Biology and Ecology, Faculty of Science, P.J. Šafárik Unversity in Košice, Mánesova 23, SK-04001, Košice, Slovakia
[b] Departamento de Bioquímica Vegetal y Biología Molecular, Facultad de Química, Universidad de Sevilla, C/Professor Gárcia González 1, E-41012 Seville, Spain

ARTICLE INFO

Keywords:
Flavonol decoration
Isoflavanes
Lotus corniculatus
Malonylation
Nitrogen availability

ABSTRACT

Nitrogen availability is key factor for plant metabolism and has a strong impact on the biosynthesis of secondary plant metabolites. A number of these metabolites are involved in the response to stress. In this paper, we investigated the effect of different N conditions in leaves of *Lotus corniculatus*. Low nitrogen conditions strongly enhanced the biosynthesis of phenolic compounds in leaves, inducing the expression genes encoding for key enzymes of phenolic metabolism such as phenylalanine ammonia lyase, chalcone synthase and isoflavone synthase. Kaempferol and quercetin glycosides as well as isoflavanes accumulated in leaves. Surprisingly, if the nitrogen availability was limited, but without nitrogen deprivation symptoms, an increase in the levels of phenylpropane acids and a decrease in the levels of kaempferol glycosides was detected. Especially the decrease in malonylated kaempferol derivatives and the kaempferol glycosides substituted by rhamnose in the 3-O position. The *L. corniculatus* malonyltransferase 1 gene is likely involved in the malonylation of the kaempferol glycosides.

1. Introduction

The biosynthesis of phenolic compounds is one of the main secondary routes in plant metabolism. Phenolic compounds play several roles in plant metabolism and in the response to stress conditions, and several of these compounds have potential pharmacological value. Phenolic compounds are the most widely distributed secondary metabolites even if the type of compound present may vary depending on the plant taxa (Cheynier et al., 2013). These metabolites are involved in the pigmentation of flowers and seeds, protection to UV irradiation, protection to oxidative damage caused by abiotic or biotic stress factors of interaction with symbiotic organisms.

Nitrogen is a crucial plant macronutrient that is also involved in the balance between growth and the flux towards secondary metabolism pathways (Lillo et al., 2008). The availability and form of nitrogen can significantly impact plant growth. Nitrate stimulates the lateral root growth that depends on the perception by the lateral root tip, which is under the control of NPF6.3 (formerly known as NRT1.1), a nitrate sensor with auxin transport activity (Wen and Kaiser, 2018; Bouguyon et al., 2015). Similarly to the closely related *L. corniculatus*, the model plant, *L. japonicus*, prefers the combined N nutrition (nitrate + ammonia) and is a root nitrate assimilator (Prosser et al., 2006; Márquez et al., 2005). An increase in external nitrate concentration up to 24 mM does not lead to a substantial change in the root/shoot partitioning of nitrate assimilation (Márquez et al., 2005). On the other hand, increasing ammonium concentration up to 20 mM significantly inhibits the elongation of primary and lateral roots, without affecting the biomass of the shoot (Rogato et al., 2010). Assimilated nitrogen is then transported from root to shoot in the form of asparagine, which is the main nitrogen source for the shoot (García-Calderón et al., 2017).

N availability regulates the transport and partitioning of metabolites produced in photosynthesis between the primary and secondary metabolism in plants (Fernie et al., 2020). Low nitrogen availability was found to increase the accumulation of phenolic compounds in plants (Rubio-Wilhelm et al., 2012). Since the C and N content in plants is coordinated, a high C/N ratio is supposed to generate a shift from nitrogen to carbon-based metabolites (Deng et al., 2019; Rubio-Wilhelm et al., 2012) that can increase the antioxidative defence capacity in cells. Moreover, phenolic compounds are synthesised by the action of phenylalanine ammonia lyase (PAL) that releases ammonia from

* Corresponding author.
E-mail address: peter.palove-balang@upjs.sk (P. Paľove-Balang).

https://doi.org/10.1016/j.stress.2023.100336
Received 21 July 2023; Received in revised form 18 December 2023; Accepted 27 December 2023
Available online 28 December 2023

phenylalanine substrate, producing cinnamic acid. The released ammonia increases the available nitrogen in plants. PAL is the first enzyme of phenylpropanoid pathway and is a link between primary metabolism and the biosynthesis of phenolics compounds (Larbat et al., 2012; Olsen et al., 2009; Zhang and Liu, 2015). The biosynthesis of phenolic compounds involves a sequence of central enzymatic reactions (called general phenylpropanoid pathway), from which different branch pathways lead to the production of different aromatic compounds such as lignins, coumarins or flavonoids (Naoumkina et al., 2010; Zhang and Liu, 2015). Isoflavonoids are a class of phenolic compounds that are found mainly in legumes, which have been believed to be involved mainly in adaptation to biological environment both as defensive compounds and signalling molecules in symbiotic interactions. Understanding the regulation of these processes is important for plant defence and productivity (García-Calderón et al., 2020; Kumar et al., 2020). Moreover, an increasing amount of evidence points to the involvement of isoflavonoids in the response to abiotic stress such as UV irradiation, drought, salinity or toxic metals. For this reason, the understanding and manipulation of this pathway is of great interest for improving the defence capacity of legume species in changing climatic conditions (Trush and Pal'ove-Balang, 2023). The key enzyme for the biosynthesis of both flavonoids and isoflavonoids is chalcone synthase (CHS) that is a type III Polyketide synthase that catalyses the conjugation of three acetate units from malonyl-CoA to a p-coumaroyl-CoA starter molecule produced via the general phenylpropanoid pathway (Austin et al., 2003). Induction of *CHS* gene expression in plants under stress conditions such as UV light, and bacterial or fungal infection lead to the accumulation of flavonoid and isoflavonoid compounds (Dao et al., 2011).

However, the control of the flavonoid and isoflavonoid branches of the phenolic pathway that results in different accumulation patterns of their end-products is far from being completely understood. Plant nitrogen status is one of the important factors that can be involved in these regulations. The present study is focused on unravelling the relationship between N availability and the expression levels of the key flavonoid-related genes as well as the regulatory function of low nitrogen status in plants on flavonoid and isoflavonoid accumulation in the forage legume, *L. corniculatus*. For this purpose, the available sequence data in the close related model plant, *L. japonicus* were exploited. The results can give a better insight into the changes in biosynthesis of defensive and often biologically active substances in leaves at the different plant N-status.

2. Material and methods

2.1. Plant material and growth conditions

Lotus corniculatus L. cultivar (cv.) 'INIA Draco' (Uruguay) was selected as experimental material due to its good growth and its high flavonoid content. All treatments included 25 seedlings each. Seedlings were propagated by 8 cm shoot cuttings transferred to pots (5 cuttings per pot) filled with Vermiculite. Plants were grown for 30 d at photosynthetic photon flux density at the plant level about 150 μmol m^{-2} s^{-1} (4000 K) under a 16/8 h day/light cycle, at 22 °C with 70 % relative humidity. Pots were watered with standard Hornum nutrient solution as described in Handberg and Stougaard (1992) containing 3 mM KNO_3 and 6 mM NH_4NO_3.

For experiments with different nitrogen availability, the plant roots were washed three times with distilled water and transferred to the 1/10 hydroponic solutions, while the nitrogen concentrations were adjusted as follows: 3 mM KNO_3 and 6 mM NH_4NO_3 (high nitrogen (HN) – 15 mM N in total); 0.3 mM KNO_3 and 0.6 mM NH_4NO_3 (moderate nitrogen (MN) – 1.5 mM N in total); 0.015 mM KNO_3 and 0.03 mM NH_4NO_3 (low nitrogen (LN) – 0.075 mM N in total). The solutions were changed every 3 days for 15 days.

2.2. Chlorophyll, carotenoid content and maximum quantum yield

For chlorophyll and carotenoid estimation, 0.1 g of fresh leaves from the shoot tip (2nd to 3rd leaves) were homogenised in a mortar with 10 ml of absolute methanol and 1 mg of MgCO3 in the dark. The crude extracts were centrifuged for 10 min at 4000 rpm to remove the insoluble material. The absorbance was measured at 470, 653, 666 and 750 nm using a spectrophotometer Jenway 7310 with 1 nm resolution. Carotenoid, chlorophyll a and b contents were calculated according to Wellburn (1994) equations. The maximum quantum yield for PSII (Qv) in 30 min dark-adapted leaves was calculated as the ratio of variable and maximum fluorescence (Fv/Fm) using FluorCam 800MF.

2.3. RNA extraction and real-time PCR

Total RNA was isolated from *L. corniculatus* leaves using the protocol described by Kistner and Matamoros (2005). A biological replicate consisted of the leaves from two plants grown in the same pot pooled together. Three independent biological samples for each condition were used for RNA extractions. The integrity and concentration of the RNA were checked by electrophoresis (Bio-rad Power Pack Basic) as well as using a fluorescent microplate reader Biotek Synergy HT (Bio-Rad). For qRT-PCR analysis, total RNA was treated with the TURBO DNA-free DNAse (Ambion). Reverse transcription was performed with Thermo Scientific RevertAid Reverse Transcriptase using 1 μmol of total RNA extract and oligo dt: (dt)12GN, (dt)12CN, (dt)12AN-(1:1:1) (Sigma). DNA contamination and RNA integrity were checked by qRT-PCR reaction with oligonucleotides that amplified an intron in the *L. japonicus* hypernodulation aberrant root formation (*LjHAR1*) gene and the 5′ and 3′ ends of the *L. japonicus* glyceraldehyde-3-phosphate dehydrogenase respectively (using the oligonucleotide pair *LjGAPDH5'* and *LjGAPDH3'*). qRT-PCR reactions were carried out in a 20 μL final volume with Light Cycler® Nano Roche using a FastStart Essential DNA Green Master kit (Roche). 2^{-Ct} values were standardized by dividing them by the geometric mean of 2^{-Ct} values of the genes encoding for *L. japonicus* polyubiquitin4 (*LjUBQ4*) and protein phosphatase 2A reg. subunit (*LjPP2A*), which were selected from the most stably expressed genes in the plants (Czechowski et al., 2005; Sánchez et al., 2008).

Gene-specific oligonucleotides were designed for 13 genes encoding for chalcone synthase, 3 genes for Malate dehydrogenase, 12 genes for UDP-glycosyltransferase with putative involvement in flavonoid glycolysation (Krishnamurthy et al., 2020), according to Lotus Base (Mun et al., 2016). Gene-specific oligonucleotides for PAL were designed previously (Trush et al., 2023). A list of all oligonucleotides used is provided in Supplemental.

As the oligonucleotides were designed according to the *L. japonicus* genome and used for the related species *L. corniculatus*, the Sanger sequencing was performed on the qPCR products and the corresponding sequences from *L. japonicus* genome were compared for identity.

2.4. Chromatographic analysis and MS identification of flavonoids and isoflavonoids

All leaves from one individual plant were used for each biological replicate. Leaves were dried gently for 24 h at 50 °C and stored in the dark in a desiccator at room temperature until use. Such treatment did not cause a significant change in the main flavonoid profiles in *L. japonicus* (García-Calderón et al., 2015). 50 mg of dry tissue was extracted with 1.5 mL of 80 % (v/v) methanol. Samples were centrifuged shortly and filtered through a 2 μm membrane. The samples were analysed by gradient reversed phase HPLC using an Agilent 1260 Infinity Quaternaly LC system with 1260 Infinity DAD detector (Agilent Technologies, USA) and Arion© Polar C_{18} 250 × 4.6 mm 5 μm column. The solvent was delivered to the column at a 0.7 mL min^{-1} flow rate. A gradient system with two mobile phases was used; 5 % acetonitrile with 3 % trifluoroacetic acid (A) and 80 % acetonitrile (B). The gradient

programme utilised for determination of flavonoids was as follows: 0 min A/B (90:10); 5 min A/B (86:14); 30 min A/B (76:24); 35 min A/B (60:40); 50 min A/B (0:100); 55 min A/B (0:100); 60 min A/B (90:10). The gradient programme utilised for determination of isoflavonoids was as follows: 0 min A/B (90:10); 5 min A/B (60:40); 24 min A/B (0:100); 30 min (0:100); 35 min (90:10). Compounds were detected at 220 and 350 nm.

Chromatographic peaks were identified based on their retention time and UV–Vis spectra measurements carried out during the analysis and also according to the MS data available from previous analyses (Kaducová et al., 2022). Commercially available standards were employed; vestitol (Biorbit), quercetin-3-O-rhamnoside (Extrasynthese), kaempferol-3-O-glucoside, kaempferol-3-O-rhamnoside, *p*-Coumaric acid, *p*-Ferulic acid, Cinnamic acid (Sigma Aldrich)

For quantification, kaempferol-3-O-glucoside was used as the reference for MS identified kaempferol glycosides, quercetine-3-O-rhamonside for quercetin glycosides and vestitol was used as the reference for its derivative and sativan. All flavonols were evaluated at $\lambda =$ 350 nm, vestitol, vestitol derivative, sativan at $\lambda = 220$ nm, coumaric acid, ferulic acid, cinnamic acid at $\lambda = 280$ nm and their content was expressed as μmol g^{-1} dry mass.

2.5. Anthocyanidins and tannin content

Anthocyanidin and tannin levels were determined in all leaves of individual plant pooled together. Samples were extracted overnight in 2 ml of methanol acidified with 1 % HCl. After the addition of 1.4 mL of distilled water, anthocyanins were separated from chlorophylls with 3.5 mL of chloroform and centrifuged 5 min. at 10,000 rpm. Total anthocyanins were determined by measuring the absorbance at $\lambda = 530$ nm and 657 nm of the aqueous phase using a spectrophotometer (Jenway 6705 UV/VIS). The relative amount of anthocyanin per seedling was calculated by subtracting the absorbance at 657 nm from the absorbance at 530 nm (Neff and Chlory, 1998) and the result was expressed as the relative amount of anthocyanin per seedling. The tannin content was estimated according to the Vanillin assay method described by Hagemann (2002). Catechin was used to standardize the reaction. The absorbances obtained from running the vanillin reaction in methanol were converted to "catechin equivalents" (Hagemann, 2002; Herald et al., 2014).

2.6. Phylogenetic analyses

A phylogenetic tree was constructed using the protein-coding nucleotide sequences of 1 AtCHS, 18 MtCHSs, 17 GmCHSs and 13LjCHSs as well as 4 NtCHS and 1 OsCHS, the latter used as outgroup. *Lotus japonicus* represents self-compatible diploid species morphologically distinguished from tetraploid outcrosser *L. corniculatus* (Barykina and Kramina, 2006; Cheng and Grant, 1973). Both species are evolutionary very closely related (Degtjareva et al., 2008) and their tetraploid forms are interfertile (Hashiguchi et al., 2017). In fact, *L. japonicus* was not recognised as separate species in some taxonomic concepts and referred as *L. corniculatus* subsp. *japonicus* (Regel) H.Ohashi (Iwatsuki et al., 2001). Therefore, the phylogenetic tree constructed with *L. japonicus* sequences may be employed for the interpretation of the results determined in *L. corniculatus*. The nucleotide sequences were aligned using ClustalW multiple alignment method in MEGA11 ver. 11.0.13 (Tamura et al., 2021), then checked by eye for positions of indels, and finally trimmed. Substitution model GTR+Γ was determined as the best fitted the data based on the Akaike information criterion in jModeltest ver. 2.1.9 (Darriba et al., 2012). Phylogenetic relationships between sequences and tree reconstruction were conducted applying Bayasian inference (BI) methods implemented in MrBayes ver. 3.2.7 (Ronquist et al., 2012). The BI analysis with Markov chain Monte Carlo algorithm was performed with 2 runs, each with four chains, and with trees sampled every 500 generations from a total of 5,000,000 generations. Potential scale reduction factor approaching 1.0 suggests convergence of both runs. Further convergence diagnostics of BI was done in Tracer ver. 1.7.2 (Rambaut et al., 2018) and showed that the log probability starts to plateau and both runs turn to converge early after start of BI analysis. Therefore, a majority-rule consensus tree was computed excluding 10 % of all sampled trees (burn-in phase).

2.7. Statistical and data analysis

Significant differences between the three nitrogen treatments were determined for the gene expression levels, metabolite accumulation and physiological parameters using ANOVA with a post hoc Tukey's HSD test. The number of repetitions and *p*-values are indicated in tables and figures.

3. Results

3.1. Physiological parameters and metabolite accumulation

Physiological parameters were determined in three different nitrogen statuses: HN, representing high nitrogen conditions with a sufficient nitrogen supply; MN, signifying moderate nitrogen conditions with a limited nitrogen supply but without marked nitrogen deficiency stress; and LN, representing low nitrogen conditions, where a decrease in nitrogen in the plants also led to nitrogen deficiency stress symptoms.

A decrease in nitrogen availability in *L. japonicus* in LN resulted to the significant decrease of total nitrogen as well as nitrate content in leaves (Table 1). On the other hand, in plants on MN, the internal nitrogen and nitrate content was similar to plants in HN conditions. Chlorophyll *a* and *b*, carotenoid content as well as the Fluorescence quantum yield showed similar patterns (Table 1). On MN conditions all measured parameters tended to decrease but were still very similar to those determined in the plants on HN availability, whereas they strongly decreased on LN.

Nitrogen availability strongly affected the accumulation of different phenolic compounds in *L. corniculatus* leaves. On MN, there was a high increase in ferulic and cinnamic acid content, whereas levels of coumaric acid were not clearly affected in comparison to plants under HN conditions (Table 2). The overview of the biosynthetic pathways studied in the present work is presented on Fig. S1. The levels of the most abundant kaempferol-glycosides decreased, while others tended to increase, or their levels were unchanged (Table 2). The glycosylation of kaempferol occurs mainly at the 3- and 7-O-positions. The kaempferol glycosides substituted by 6-deoxyhexose (rhamnose) at position 3, namely kaempferol-3,7-O-dirhamnosid, kaempferol-6-deoxyhexose, −6-deoxyhexose, -malonyl and kaempferol-3-O-rhamnosid levels strongly decreased (Table 2). The first two compounds were also the most abundant kaempferol glycosides in leaves. High levels of the malonylated kaempferol glycoside is typically present in *L. corniculatus* cv. INIA Draco and it has been further described before (Kaducová et al.,

Table 1
Total nitrogen, nitrate, chlorophyll, carotenoid content and fluorescence quantum yield (Qv) in the leaves of plants treated with different levels nitrate. Values are the means of 4 biological replicates ± SE. Different letters indicate significant difference between treatments based on ANOVA with post-hoc Tukey HSD test ($p < 0.05$).

	High nitrate	Moderate nitrate	Low nitrate
Total N (mg/g DW)	47.32 ± 1.09^{b}	45.10 ± 1.43^{b}	17.67 ± 0.55^{a}
Nitrate (μmol/g FW)	3.25 ± 0.08^{b}	2.81 ± 0.51^{b}	0.43 ± 0.19^{a}
Chl a (mg/g FW)	2.87 ± 0.20^{b}	2.81 ± 0.19^{b}	1.77 ± 0.11^{a}
Chl b (mg/g FW)	0.55 ± 0.04^{b}	0.48 ± 0.09^{ab}	0.33 ± 0.02^{a}
Carotenoids (mg/g FW)	0.88 ± 0.04^{b}	0.84 ± 0.06^{b}	0.58 ± 0.03^{a}
Fluorescence quantum yield - Qv	0.746 ± 0.007^{b}	0.738 ± 0.002^{b}	0.691 ± 0.003^{a}

Table 2
Effect of nitrogen availability on phenolic compounds content in *L. corniculatus* leaves. Data are means in μmol g^{-1} DM ± SE (italic) of 4 biological replicates. Different letters indicate significant difference between treatments based on ANOVA with post-hoc Tukey HSD test ($p < 0.01$).

Compound	*HN*	*MN*	*LN*
Kaempferol-3-O-glucosyl (1-2)-galactoside-7-O-rhamnoside	0.030 ± *0.007*^{a}	0.031 ± *0.003*^{a}	0.062 ± *0.002*^{a}
Kaempferol-6DH, -Hex, -Pen	0.145 ± *0.005*^{a}	0.226 ± *0.009*^{a}	0.159 ± *0.018*^{a}
Kaempferol-6DH, -Hex-Pen	0.091 ± *0.007*^{a}	0.092 ± *0.017*^{a}	0.101 ± *0.016*^{a}
Kaempferol-3-O-galactosyl-7-O-rhamnoside	0.099 ± *0.016*^{a}	0.174 ± *0.013*^{a}	0.126 ± *0.024*^{a}
Kaempferol-3-O-glucosyl-7-O-rhamnoside	0.496 ± *0.066*^{a}	0.675 ± *0.158*^{a}	0.656 ± *0.080*^{a}
Kaempferol-3,7-di-O-rhamnoside	1.523 ± *0.063*^{b}	0.522 ± *0.107*^{a}	2.220 ± *0.100*^{c}
Kaempferol-6DH, -6DH, - Mal	1.618 ± *0.065*^{b}	0.735 ± *0.136*^{a}	2.153 ± *0.124*^{c}
Kaempferol-3-O-rhamnoside	0.048 ± *0.003*^{b}	0.015 ± *0.004*^{a}	0.073 ± *0.004*^{c}
Kaempferol-3-O-glucoside	0.036 ± *0.004*^{a}	0.022 ± *0.004*^{a}	0.063 ± *0.001*^{b}
Kaempferol-7-O-6DH	0.092 ± *0.006*^{a}	0.226 ± *0.004*^{b}	0.084 ± *0.008*^{a}
Quercetin -6DH, -6DH	0.056 ± *0.005*^{a}	0.140 ± *0.049*^{a}	0.272 ± *0.039*^{b}
Coumaric acid	0.303 ± *0.024*^{ab}	0.242 ± *0.035*^{a}	0.386 ± *0.019*^{b}
Ferulic acid	0.565 ± *0.034*^{a}	1.389 ± *0.263*^{b}	0.585 ± *0.065*^{a}
Cinnamic acid	0.036 ± *0.003*^{a}	0.067 ± *0.004*^{b}	0.044 ± *0.004*^{a}
Vestitol	0.259 ± *0.043*^{a}	0.323 ± *0.040*^{a}	0.889 ± *0.155*^{b}
putative isoflavan Sativan	0.124 ± *0.017*^{a}	0.140 ± *0.054*^{a}	0.722 ± *0.401*^{b}
Total condensed tannins (μmol catechin equivalents g^{-1} DM)	8.19 ± *0.82*^{a}	6.30 ± *0.70*^{a}	6.78 ± *0.69*^{a}
Relative anthocyanidins (A530−A657) × 1000 $seedling^{-1}$	5.21 ± *0.40*^{a}	6.36 ± *0.51*^{a}	5.71 ± *0.92*^{a}

6DH, 6-deoxyhexose; Hex, hexose; Pen, pentose; Mal, malonyl.

2022). On the other hand, those kaempferol compounds that are substituted at position 3 by hexose (glucose or galactose) were not affected or tended to increase on MN conditions. The total amount of substance per gram of dry mass of all glycosides substituted at position 3 by hexose significantly increased by more than 50 % (Fig. 1). However, this increase was not significant if the compounds were calculated individually, likely due to quite high variability between replicates (Table 2). The only significant increase was found in the case of kaempferol-7-O-6-deoxyhexose that is not substituted at the position 3.

On LN conditions, the kaempferol glycosides substituted at position 3 by 6-deoxyhexose (rhamnose) significantly increased in comparison to HN but even more in comparison to MN conditions (Table 2). The levels of the other kaempferol glycosides under HN and LN conditions were very similar. The decrease of nitrogen availability also induced the accumulation of vestitol and sativan (Table 2).

The anthocyanidin levels in plant were overall very low and were not markedly affected by nitrogen. The tannin content was neither significantly affected by nitrogen, although tended to be slightly higher under HN conditions (Table 2).

3.2. Expression and activity of phenylalanine ammonia lyase

The expression levels of the genes encoding for PAL, the enzyme that links primary metabolism and the biosynthesis of phenolic compounds, were determined by qRT-PCR. The expression of the 12 different isogenes present in the Lotus genome was measured in leaves of *L. corniculatus*. The gene code number was appointed according to previous works (Chen et al., 2017; Trush et al., 2023). To confirm the identity of the qPCR products, their were sequenced and their sequence was compared to *L. japonicus* (ecotype MG-20). High sequence identities were found (Table S2). The qPCR product of *LcPAL10* showed high (99.37 %) identity to the gene *LotjaGi5g1v0102000.1* that is present in the genome of *L. japonicus* ecotype Gifu (B-129-S9), whereas in other ecotype MG20, the ortholog sequence *Lj0g3v0350889.1* contain a 33 bp gap (Lotus BASE, 2022; Mun et al., 2016).

Among the measured isogenes, for four of them no expression was detected in leaves. Expressions of *LcPAL2, LcPAL5, LcPAL6* and *LcPAL7* were not significantly affected by nitrogen (Fig. 2). *LcPAL6* showed a high relative expression rate, but also high variability. Relative expression rates of the *LcPAL4, LcPAL8, LcPAL9* and *LcPAL10* increased significantly on LN, with the latter two being the most highly expressed PAL genes under these conditions. The enzymatic activity of PAL was also measured in order to confirm the qPCR data. PAL enzyme activity was lower on HN conditions compared to MN and LN conditions (Fig. 3).

3.3. Expression of chalcone synthase

Chalcone synthase (CHS), the key enzyme for flavonoid biosynthesis, is encoded by at least 14 different genes, according to the data available for the Lotus genome. As many as 12 of them were found to be expressed in leaves of *L. corniculatus* (Fig. 4). The qPCR products of most of them

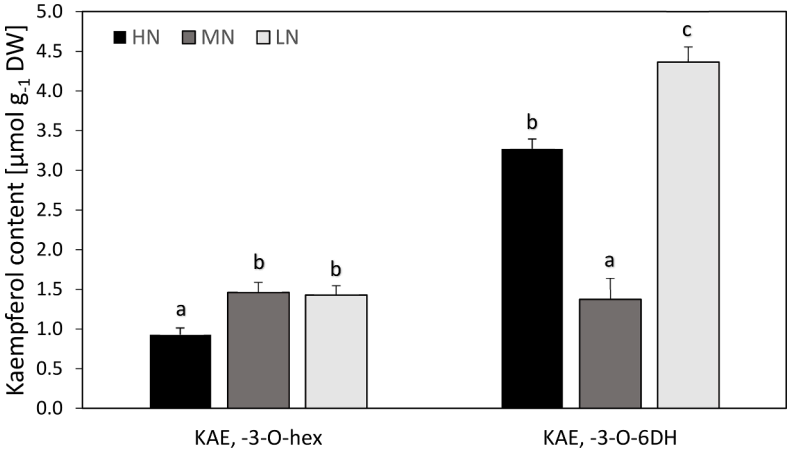

Fig. 1. Accumulation of kaempferol glycosides at high (HN), medium (MN) and low nitrogen availability (LN) in leaves. Results are means of the sum of all kaempferol glycosides substituted with hexoses (KAE 3-O-hex) or 6-deoxyhexoses (KAE 3-O-DH) of four biological replicates + SE. Different letters indicate significant difference between treatments based on ANOVA with post-hoc Tukey HSD test ($p < 0.05$).

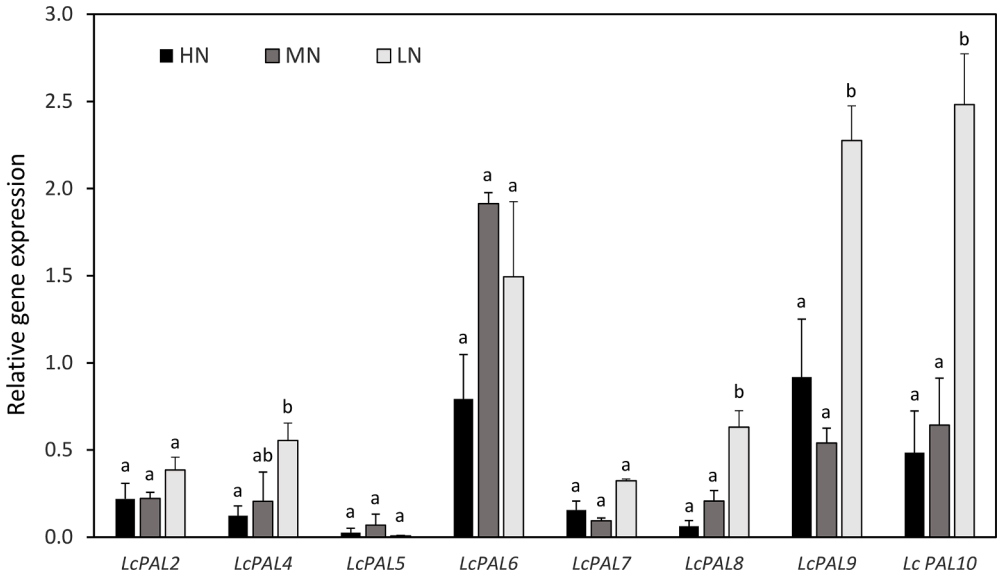

Fig. 2. Relative expressions levels of phenylalanine ammonia lyase (PAL) genes at high (HN), medium (MN) and low nitrogen availability (LN). The values are the means of the genes expression levels relative to the combined housekeeping genes *Lj*PP2A and *LjUBQ4* (+SE) from three biological replicates. Different letters indicate significant difference based on ANOVA with post-hoc Tukey HSD test ($p < 0.05$).

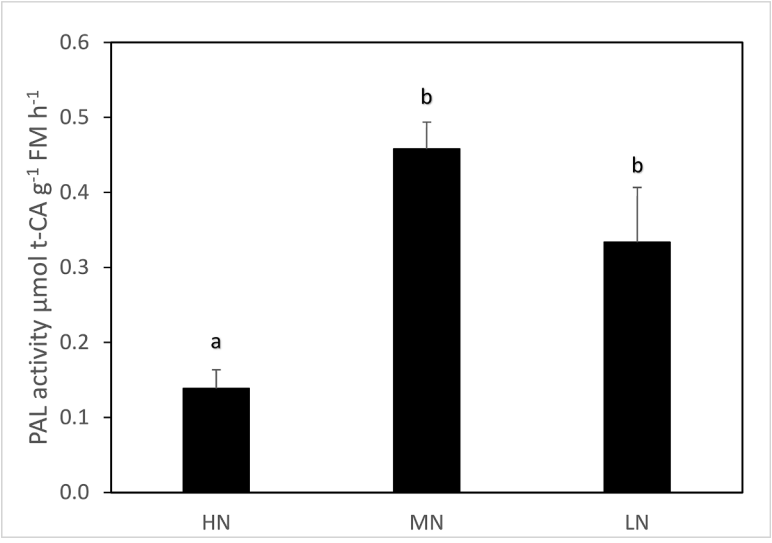

Fig. 3. Effect of the high (HN), medium (MN) and low nitrogen availability (LN) on the PAL enzyme activity in leaves. PAL activity was determined as the production of t-cinnamic acid (t-CA). The data are the means of 4 biological replicates + SE. Different letters indicate significant difference between treatments based on ANOVA with post-hoc Tukey HSD test ($p < 0.05$).

showed high identity to the corresponding genes in *L. japonicus* genome (Table S2). The two exceptions were *LcCHS9* and *LcCHS14*, which showed lower identity (91.4 % to Lj2g3v2124320.1 and 92.05 % to Lj6g3v0933570.1 respectively). The main reason is a 5 bp gap in the Lj2g3v2124320.1 in comparison to the corresponding qPCR product and 6 bp gap in the Lj6g3v0933570.1.

LcCHS3 and *LcCHS6* showed the highest expression rates on moderate nitrogen but were not predominant in leaves. A phylogenetic tree constructed using the protein-coding sequences from *Lotus japonicus, Glycine* max, *Medicago truncatula, Nicotiana tabacum, Arabidopsis thaliana*, and *Oryza sativa* showed that *LjCHS3* and *LjCHS6* are distantly related to other Lotus CHS genes (Fig. S2) and *LjCHS6* was closer to soybean *GmCHS13* and *LjCHS3* to *GmCHS14*. These results suggest that *LjCHS3* and *LjCHS6* may have different function compared to the other *LjCHS* genes. The genes *LjCHS12* and *LjCHS13* fell also in separate group together with most of the *GmCHS* genes, whereas *LjCHS1, LjCHS4, LjCHS5, LjCHS7, LjCHS9, LjCHS10, LjCHS11* and *LjCHS14* have a very similar sequences to each other and fell into same group to the most of the *MtCHS* genes. Under LN conditions the expression of *LcCHS9, LcCHS10, LcCHS11, LcCHS12* and *LcCHS13* increased (Fig. 4). *LcCHS11* was the most expressed gene followed by *LcCHS10, LcCHS12*, and others. *LcCHS9, LcCHS10* and *LcCHS11* are phylogenetically closely related (Fig. S1), and they orthologs from *L. japonicus* are localised on the chromosome 2. The ortholog of *LcCHS12* is located on the chromosome 4 in *L. japonicus* genome together with the phylogenetically close-related *LjCHS13*. Expression of *LcCHS2, LcCHS4, LcCHS5, LcCHS7* and *LcCHS14* was not affected by nitrogen levels.

Expression of isoflavone synthase

Isoflavone synthase (IFS) is a key enzyme in the synthesis of isoflavones. The expression of the genes encoding for isoflavone synthase

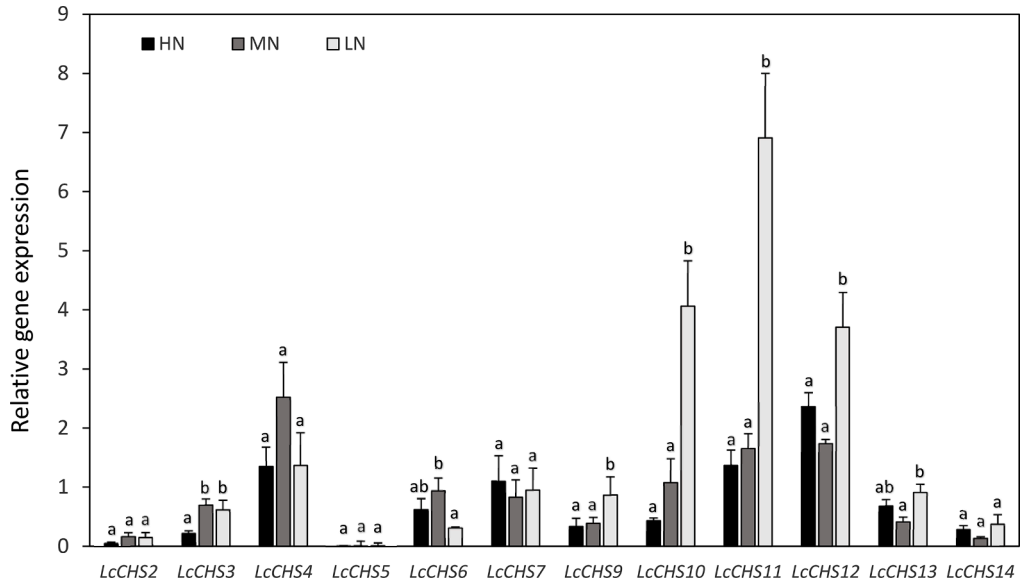

Fig. 4. Relative expressions levels of chalcone synthase (CHS) genes at high (HN), medium (MN) and low nitrogen availability (LN). The values are the means of the genes expression levels relative to the combined housekeeping genes *Lj*PP2A and *LjUBQ4* (+SE) from three biological replicates. Different letters indicate significant difference based on ANOVA with post-hoc Tukey HSD test ($p < 0.05$).

isoform 1 and 3 (*LcIFS1, LcIFS3*) significantly increased on LN, although the expression rate of *LcIFS1* was low (Fig. 5). The identity of both qPCR products was high compared to the corresponding sequences in *L. japonicus* genome (Table S2). The expression levels of *LcIFS2* were undetectable.

3.5. Expression of flavonol-malonyltransferase and UDP-glycosyltransferases

A search of the genome database Lotus Base (Mun et al., 2016) was conducted to identify genes that may be involved in flavonoid-malonylation based on sequence homology to characterized malonyltransferases from other plant species. Three candidate genes were found and designated *LcMaT1, LcMaT2*, and *LcMaT3* (Table S1) according to their orthology to *Medicago truncatula*. Increase of kaempferol-6DH, -6DH, -Mal was paralleled by an increase of expression of *LcMaT1*, (Fig. 5) whereas the expression of *LcMaT2* and *LcMaT3* was undetectable.

The genes encoding for UDP-glycosyltransferase (UGT) were chosen according their putative flavonol-glycosilation activities. *LcUGT78D1* and *LcUGT78D2* are the orthologs of the *Arabidopsis* genes providing the 3-O-rhamnosylation and/or 3-O glucosylation activities (Kim et al., 2013; Yonekura-Sakakibara et al., 2008). The expression levels of other genes of UGT72 and UGT73 families that were described to be flavonoid related (Jones et al., 2003; Krishnamurthy et al., 2020; Yin et al., 2017) were also measured. The nomenclature of the UGT genes was kept according to Yin et al. (2017) and following rules described in Ross et al. (2001), the gene-sequence codes were updated according to the Myjakogusa.jp (2022) 3.0 database (Table S1). The DNA sequence of the PCR products was determined for all the Mal and UGT genes. All of the PCR products of *UGT* and *Mal* genes showed high similarity to the corresponding sequences available in the *L. japonicus* genome (Table S2).

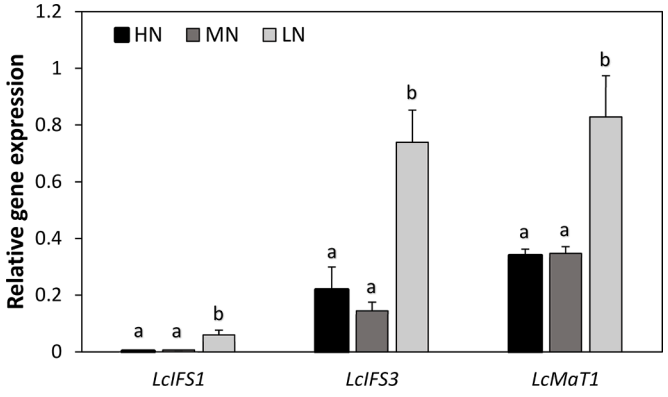

Fig. 5. Relative expressions levels of isoflavone synthase (IFS) and malonyltransferase (*MAL*) genes at high (HN), medium (MN) and low nitrogen availability (LN). The values are the means of the genes expression levels relative to the combined housekeeping genes *Lj*PP2A and *LjUBQ4* (+SE) from three biological replicates. Different letters indicate significant difference based on ANOVA with post-hoc Tukey HSD test ($p < 0.05$).

The expression levels of *UGT* genes were generally quite low (Fig. 6). No expression was detected for *LcUGT73C6, LcUGT72AD1, LcUGT72AE1 and LcUGT79D2* in leaves. Different nitrogen availability resulted only to small changes in UGT expression rates. *LcUGT72V2, LcUGT72AF1 and LcUGT79B30* were not affected by nitrogen levels. The expression of *LcUGT73B2, LcUGT73C17 and LcUGT78D1* tended to increase on MN and decrease on HN. However, such changes were significant only for *LcUGT73B2* (Fig. 6). *LcUGT72AH1* had the highest expression rate on HN, whereas MN and LN conditions significantly decreased its expression.

4. Discussion

Plant nitrogen status has a strong influence to flavonoid-metabolism and accumulation of the end products. In particular, nitrogen deficiency lead to flavonoid accumulation, mainly flavonols and anthocyanidins, and induces the expression of genes encoding for biosynthetic enzymes of phenolic pathway (Becker et al., 2015; Larbat et al., 2012; Lillo et al., 2008). In the present work, we showed that nitrogen availability had a strong impact on phenolic metabolism in *L. corniculatus* leaves. Despite the fact, that MN conditions did not cause nitrogen deficiency symptoms, different branches of phenolic pathway were modulated in comparison to HN. The enzyme activity of PAL increased and resulted in enhanced accumulation of ferulic acid. The levels of cinnamic acid, the product of PAL reaction, also significantly increased. The results suggest higher production of phenylpropanoid acids via the general phenypropanoid pathway, whereas biosynthesis of flavonoids is not induced. On

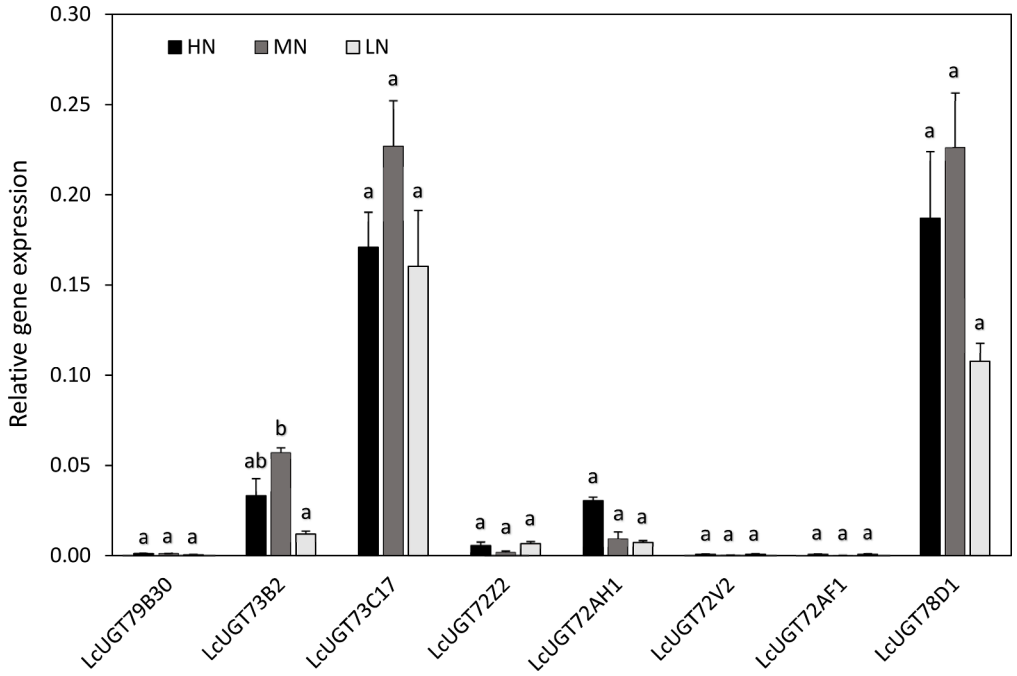

Fig. 6. Relative expressions levels of UDP-glucosyltransferase genes; *UGT79B6* (79B6), *UGT73B2* (73B2), *UGT73C5* (73C5), *UGT72B1* (72B1), *UGT72AH1* (72AH1), *UGTAF1* (AF1), *UGT72B3* (B3) and *UGT78D1* at high (HN), medium (MN) and low nitrogen availability (LN). The values are the means of the genes expression levels relative to the combined housekeeping genes *Lj*PP2A and *LjUBQ4* (+SE) from three biological replicates. Different letters indicate significant difference based on ANOVA with post-hoc Tukey HSD test ($p < 0.05$).

LN conditions high PAL activity resulted in enhanced production of vestitol and sativan and of kaempferol glycosides end- products. Quercetin glycoside also significantly increased. In soybean, low nitrogen conditions also stimulated the phenylpropanoid pathway, and increased isoflavonoid production, whereas the biosynthesis of flavonoids was suppressed without strong effect on flavonoid accumulation in leaves (Nezamivand-Chenini et al., 2022). However, the 0.5 mM nitrogen used for soybean was more similar to the MN conditions in the present work, whereas nitrogen availability was much more limited on LN.

PAL is not only the link between primary metabolism and the biosynthesis of phenolic compounds but is also of special interest in relation to nitrogen nutrition because it releases nitrogen from phenylalanine, and thereby makes nitrogen available for redistribution (Lillo et al., 2008). In nitrogen limitation, expression of PAL is induced (Deng et al., 2019; Larbat et al., 2012; Lillo et al., 2008). Four *PAL* isogenes are present in *Arabidopsis.* The expression of *AtPAL1* and *AtPAL2* is inducible by nitrogen depletion and is supposed to play a role in environmentally triggered phenolic synthesis (Olsen et al., 2009; Zhang and Liu 2015). Among the 12 *PAL* isogenes tested in *L. corniculatus* leaves, four of them (*LcPAL4, LcPAL8, LcPAL9* and *LcPAL10*) were significantly induced under LN conditions (Fig. 2). However, on MN no clear increase of *PAL* expression was determined, so the increase in PAL activity in such condition was not regulated at the transcription level. Instead, a post-translational regulation can be suggested. Increase of PAL activity on MN was not accompanied with increase in flavonoid compounds, but rather with increased accumulation of phenylpropanoids that may also be related to the changes in biosynthesis of lignin and/or other related compounds. The impact of N-status on lignin production has been reported in different species (Rivai et al., 2021; Zhang et al., 2017). However, this point has not been investigated in detail in the present work and need further investigation to elucidate the underlying mechanisms. Despite this, the results support the view that the general metabolic response of plants to LN and MN conditions is different.

Chalcone synthase (CHS) catalyzes the initial step in the biosynthesis of flavonoids. The high number (14) of isogenes present in *L. japonicus* is likely related to the presence of the isoflavonoid pathway and is typical for the family Fabaceae (García-Calderón et al., 2020; Zavala et al., 2015). In a similar way to *PAL*, the expression of CHS was also strongly induced on LN. This induction was more pronounced in the case of *LjCHS10, LjCHS11* and *LjCHS12* (Fig. 5). Moreover, the expression levels of *LjIFS1* and *LjIFS3* were also increased under these conditions (Fig. 6). In general, the increase of *PAL* and *CHS* expression on LN suggest the increased biosynthesis of flavonoids, and increased *IFS* expression is in agreement with the observed accumulation of isoflavonoids, especially vestitol. In soybean, the interaction of GmCHS1 with CHI and IFS suggests that this protein is involved in legume-specific isoflavonoid biosynthesis (Waki et al., 2016). *GmCHS1* is in the same clade as *LjCHS12* (Fig. S2). On the other hand, GmCHS7 has much weaker interaction with IFS implying that strength of protein-protein interactions of enzymes may vary among paralogous members and are different in their regulation and physiological roles (Waki et al., 2016).

On MN and HN conditions the expression levels of *CHS* and *IFS* were very similar for most of the isogenes. Only few genes encoding for CHS (namely *LcCHS3* and *LcCHS6*) with relatively low expression levels were induced on MN conditions. As a result, the flavonoid accumulation on MN conditions was similar, or rather lower compared to HN conditions. *GmCHS14*, that belongs a distinct clade together with *LjCHS3,* was found to be involved in isoflavonoid biosynthesis interacting with GmMYB176 regulatory transcription factor (Anguraj Vadivel et al., 2018).

In *L. corniculatus* plants collected from the field, quercetin glycosides are present in considerable amount, whereas plants grown in plant chamber usually contain very limited quercetin glycosides levels (Paľove-Balang et al., unpublished results). The possible reason is that quercetin accumulation is strongly induced by different environmental factors. In *Arabidopis*, quercetin accumulation was induced more than kaempferol by nitrogen deprivation, and low temperature (10 °C) also strongly induced quercetin accumulation (Olsen et al., 2009). However, quercetin glycosides not always accumulate more in response to external factors in comparison to kaempferol glycosides, such effect may be species specific (Neugart and Bumke-Vogt, 2021). In *L. japonicus*, quercetin glycosides were induced mostly under drought conditions, and to some extent also by salt stress (García-Calderón et al., 2015;

Mrázová et al., 2017). Other external factors such as UV and metal toxicity often induced the production of vestitol, which is an important metabolite of the isoflavonoid subgroup typically produced in the *Lotus* sp., with relevant antioxidant properties (Kaducová et al., 2019; Trush and Pal'ove-Balang, 2023).

The levels of different kaempferol glycosides have been shown to be relatively stable in different conditions such as drought, salinity or UV-B irradiation in leaves of *L. japonicus* and *L. corniculatus* (García-Calderón et al., 2015; Kaducová et al., 2022, 2019; Mrázová et al., 2017). Nitrogen availability, however, affected not only the overall accumulation of kaempferol glycosides, but even more the glycosylation and malonylation rate of that compounds. In particular, a significant increase of kaempferol-6DH, -6DH, -Mal was observed under LN, whereas on MN its content in leaves was much lower. Malonylation of flavonols is provided by malonyltransferases belonging to the BAHD-acyltransferase superfamily (Bontpart et al., 2015; D'Auria, 2006). Malonyl residues substituted on the sugar moiety of flavonoids to potentially prevent enzymatic degradation, change their solubility, act as a signal moiety promoting the sequestration of the conjugates into vacuoles or the cell wall (Viskupicova et al., 2009; Yu et al., 2008) and makes them better UV absorbents (Tohge et al., 2016). The induction of *LjMaT1* gene indicates its possible involvement in flavonol malonylation. The expression of this gene was undetectable in *L. japonicus* that do not accumulate malonylated kaemperol glycosides, or they are present only in traces (Fig. S2; Suzuki et al., 2008) and showed only low expression rate in *L. corniculatus* variety Polom that accumulated lower levels of malonylated kaempferol glycoside in comparison to the variety INIA Draco (Fig. S3). *LjMAT1* gene showed a best BLASTn match against Medicago database (*Medicago truncatula* A17 r5.0 genome portal) to *MtMaT2* (MtrunA17_Chr7g0219241, TC107784) and to *MtMaT1* (MtrunA17Chr7g0219291, TC102229).

MtMAT1 and MtMaT2 have a high affinity to genistin as a substrate, but also to naringenin-7-O-glucoside and naringin. Flavonoid 3-O-glycosides were not metabolized by these enzymes, while kaempferol or quercetin 7-O-glycosides were not tested (Yu et al., 2008). The *AtPMaT1* (AT5G39050) gene from *Arabidopsis*, showed the best BLASTn match to *LjMaT1*. The AtPMAT1 enzyme showed malonyltransferase activity towards kaempferol 7-O-glucoside, kaempferol 3-O-glucoside, naphtol-glucosides, hydroxypregnanes, but not kaempferol 3,7-O-diglucoside. A possible function of malonylation was proposed as a key reaction to separate the mode of disposal of xenobiotics, i.e. release from the cell surface or storage in vacuoles (Taguchi et al., 2010; Tropper et al., 2021). Moreover, AtPMAT1 also catalyze the malonylation of brassinolide-23-O-Glc and so contributes to brassinolide deactivation (Gan et al., 2021).

The glycosylation has been even more affected in the present work compared to the malonylation, especially on MN. Interestingly, on MN, all the kaempferol glycosides substituted in position 3 by rhamnose strongly decreased suggesting the constrained glycosylation at this position.

Enzyme with 3-O rhamnosylation activity in *Lotus* sp. has not been described up to date. The gene encoding the enzyme with UDP-rhamnose: flavonol-3-O-rhamnosyltransferase activity in Arabidopsis is AtUGT78D1 (AT1630530), although it may use also UDP-glucose as a donor nucleoside (Jones et al., 2003; Ren et al., 2012; Yonekura-Sakakibara et al., 2008). Expression of the ortholog gene *LcUGT78D1* (Lj4g3v2058340) in *Lotus* leaves however, was not paralleled with changes in accumulation of kaempferol-3-O-rhamnosides in *L. corniculatus* (Table 2). Therefore, the present data do not support its involvement in 3-O- rhamnosylation of kaempferol even if any inhibition at the protein level cannot be ruled out. The closest gene from *M. truncatula*, MtrunA17_Chr4g0072761 (Medtr4g128690, UGT78G1) has a flavonoid 3-O-glucosyltransferase activity showing higher affinity to quercetin than kaempferol (Modolo et al., 2009). The UGT73B2 in *Arabidopsis* (product of the gene At4g34135), showed flavonol 7-O-glucosyltransferase activity that glucosylates also with a 20-fold lower activity flavonols (kaempferol and quercetin) at the 3-O-position (Lim et al., 2004). The possible ortholog gene from *L. corniculatus*, LcUGT73B2 (Lj4g3v0620420) significantly increased at medium nitrogen. However, the kaempferol is glycosylated at 7-O position mostly with rhamnose in *L. corniculatus*.

The UGT72AH1 protein in *L. japonicus*, exhibited activity toward apigenin, daidzein, and genistein (Yin et al., 2017) that are typically not present in its leaves, although e.g. daidzein may be present on abiotic stress in small amounts (Kaducová et al., 2019). The biological role of UGT72AH1 is unclear, glycosylation activity toward some minor compounds, probably isoflavonoids, can not be excluded.

In conclusion, different nitrogen availability strongly modulate the phenylpropanoid and flavonoid metabolism, accumulation and decoration. LN conditions stimulated the accumulation of kaempferol glycosides and isoflavonoids in leaves of *L. corniculatus* and induced the expression of the genes encoding for the key enzymes of this metabolism. MN availability caused an increase in phenylpropane acids and decresed the accumulation of keampferol glycosides substituted by rhamnose at the 3-O position as well as the malonylated derivatives of kaempferol. Its remain unclear which UGT gene could be involved in such changes in glycosylation. LcMaT1 is likely involved in malonylation of the kaempferol glycosides.

CRediT authorship contribution statement

Kristina Trush: Investigation, Writing – original draft, Writing – review & editing. **Martina Gavurová:** Investigation. **María Dolores Monje-Rueda:** Investigation, Methodology, Validation. **Vladislav Kolarčik:** Formal analysis, Investigation, Methodology, Software. **Michaela Bačovčinová:** Investigation, Validation. **Marco Betti:** Formal analysis, Funding acquisition, Supervision, Writing – original draft, Writing – review & editing, Project administration. **Peter Paľove-Balang:** Conceptualization, Formal analysis, Funding acquisition, Investigation, Project administration, Supervision, Validation, Writing – original draft, Writing – review & editing.

Declaration of Competing Interest

The authors declare that they have no known competing financial interests or personal relationships that could have appeared to influence the work reported in this paper.

Data availability

Data will be made available on request.

Acknowledgements

Authors acknowledges the financial support of the project VEGA 1/0291/20 from the Ministry of Education, Science, Research and Sport of the Slovak Republic, Project PID2021-122353OB-I00 (MCIN/AEI/10.13039/501100011033/ and FEDER Una Manera de Hacer Europa) and RTI-2018-093571-B100 from Ministerio de Ciencia, Innovación y Universidades, Agencia Estatal de Investigación, Spain and Fondo Europeo de Desarrollo Regional (FEDER). M.D.M-R. acknowledges a FPI fellowship (Agencia Estatal de Investigación).

Supplementary materials

Supplementary material associated with this article can be found, in the online version, at doi:10.1016/j.stress.2023.100336.

References

Anguraj Vadivel, A.K., Krysiak, K., Tian, G., Dhaubhadel, S., 2018. Genome-wide identification and localization of chalcone synthase family in soybean (*Glycine max* [L]Merr). BMC Plant Biol. 18, 325. https://doi.org/10.1186/s12870-018-1569-x.

Austin, M.B., Noel, J.P., 2003. The chalcone synthase superfamily of type III polyketide synthases. Nat. Prod. Rep. 20, 79–110. https://doi.org/10.1039/B100917F.

Barykina, R.P., Kramina, T.E., 2006. A comparative morphological and anatomical study of the model legume *Lotus japonicus* and related species. Wulfenia 13, 33–56. https://doi.org/10.1139/b06-035.

Becker, C., Urlić, B., Jukić Špika, M., Kläring, H.P., Krumbein, A., Baldermann, S., Goreta Ban, S., Perica, S., Schwarz, D., 2015. Nitrogen limited red and green leaf lettuce accumulate flavonoid glycosides, caffeic acid derivatives, and sucrose while losing chlorophylls, β-carotene and xanthophylls. PLoS One 10, e0142867. https://doi.org/10.1371/journal.pone.0142867.

Bontpart, T., Cheynier, V., Ageorges, A., Terrier, N., 2015. BAHD or SCPL acyltransferase? What a dilemma for acylation in the world of plant phenolic compounds. New Phytol. 208, 695–707. https://doi.org/10.1111/nph.13498.

Bouguyon, E., Brun, F., Meynard, D., Kubeš, M., Pervent, M., Leran, S., Lacombe, B., Krouk, G., Guiderdoni, E., Zažímalová, E., Hoyerová, K., Nacry, P., Gojon, A., 2015. Multiple mechanisms of nitrate sensing by Arabidopsis nitrate transceptor NRT1.1. Nat. Plants 1, 15015. https://doi.org/10.1038/nplants.2015.15.

Chen, Y., Li, F., Tian, L., Huang, M., Deng, R., Li, X., Chen, W., Wu, P., Li, M., Jiang, H., Wu, G., 2017. The phenylalanine ammonia lyase gene *LjPAL1* is involved in plant defence responses to pathogens and plays diverse roles in *Lotus japonicus*-Rhizobium symbioses. Mol. Plant-Microbe Interact. 30, 739–753. https://doi.org/10.1094/MPMI-04-17-0080-R.

Cheng, R.I.-J., Grant, W.F., 1973. Species relationships in the *Lotus corniculatus* group as determined by karyotype and cytophotometric analysis. Can. J. Genet. Cytol. 15, 101–115. https://doi.org/10.1139/G73-010.

Cheynier, V., Comte, G., Davies, K.M., Lattanzio, V., Martens, S., 2013. Plant phenolics: recent advances on their biosynthesis, genetics, and ecophysiology. Plant Physiol. Biochem. 72, 1–20. https://doi.org/10.1016/j.plaphy.2013.05.009.

Czechowski, T., Stitt, M., Altmann, T., Udvardi, M.K., Scheible, W.R., 2005. Genome-wide identification and testing of superior reference genes for transcript normalization in *Arabidopsis*. Plant Physiol. 139, 5–17. https://doi.org/10.1104/pp.105.063743.

D'Auria, J.C., 2006. Acyltransferases in plants: a good time to be BAHD. Curr. Opin. Plant Biol. 9, 331–340. https://doi.org/10.1016/j.pbi.2006.03.016.

Dao, T.T., Linthorst, H.J., Verpoorte, R., 2011. Chalcone synthase and its functions in plant resistance. Phytochem. Rev. 10, 397–412. https://doi.org/10.1007/s11101-011-9211-7.

Darriba, D., Taboada, G.L., Doallo, R., Posada, D., 2012. jModelTest 2: more models, new heuristics and parallel computing. Nat. Methods 9, 772. https://doi.org/10.1038/nmeth.2109.

Degtjareva, G.V., Kramina, T.E., Sokoloff, D.D., Samigullin, T.H., Sandral, G., Valiejo-Roman, C.M., 2008. New data on nrITS phylogeny of *Lotus* (*Leguminosae, Loteae*). Wulfenia 15, 35–49. https://doi.org/10.1139/b06-035.

Deng, B., Li, Y., Xu, D., Ye, Q., Liu, G., 2019. Nitrogen availability alters flavonoid accumulation in *Cyclocarya paliurus* via the effects on the internal carbon/nitrogen balance. Sci. Rep. 9, 2370. https://doi.org/10.1038/s41598-019-38837-8.

Fernie, A.R., Bachem, C.W.B., Helariutta, Y., Neuhaus, H.E., Prat, S., Ruan, Y.L., Stitt, M., Sweetlove, L.J., Tegeder, M., Wahl, V., Sonnewald, S., Sonnewald, U., 2020. Synchronization of developmental, molecular and metabolic aspects of source-sink interactions. Nat. Plants 6, 55–66. https://doi.org/10.1038/s41477-020-0590-x.

Gan, S., Rozhon, W., Varga, E., Halder, J., Berthiller, F., Poppenberger, B., 2021. The acyltransferase *PMAT1* malonylates brassinolide glucoside. J. Biol. Chem. 296, 100424 https://doi.org/10.1016/j.jbc.2021.100424.

García-Calderón, M., Pérez-Delgado, C.M., Credali, A., Vega, J.M., Betti, M., Márquez, A. J., 2017. Genes for asparagine metabolism in *Lotus japonicus*: differential expression and interconnection with photorespiration. BMC Genom. 18, 781. https://doi.org/10.1186/s12864-017-4200-x.

García-Calderón, M., Pérez-Delgado, C.M., Pal'ove-Balang, P., Betti, M., Márquez, A.J., 2020. Flavonoids and isoflavonoids biosynthesis in the model legume *Lotus japonicus*; connections to nitrogen metabolism and photorespiration. Plants (Basel) 9, 774. https://doi.org/10.3390/plants9060774.

García-Calderón, M., Pons-Ferrer, T., Mrázova, A., Paľove-Balang, P., Vilková, M., Pérez-Delgado, C.M., Vega, J.M., Eliašová, A., Repčák, M., Márquez, A.J., Betti, M., 2015. Modulation of phenolic metabolism under stress conditions in a *Lotus japonicus* mutant lacking plastidic glutamine synthetase. Front. Plant Sci. 6, 760. https://doi.org/10.3389/fpls.2015.00760.

Hagemann, A.E., 2002. The tannin Handbook. https://www.users.miamioh.edu/hagermae/(accessed 5 March 2019).

Handberg, K., Stougaard, J., 1992. *Lotus japonicus*, an autonomous, diploid legume species for classical and molecular genetics. Plant J 2, 487–496. https://doi.org/10.1111/j.1365-313X.1992.00487.x.

Hashiguchi, M., Puspasari, R., Suematsu, Y., Muguerza, M., Tanaka, H., Suzuki, A., Hoffmann, F., Akashi, R., 2017. Induction of tetraploid *Lotus japonicus* and interspecific hybridization with super-root-derived *Lotus corniculatus* regenerants. Crop Sci. 57, 2387–2394. https://doi.org/10.2135/cropsci2016.09.0743.

Herald, T.J., Gadgril, P., Perumal, R., Bean, S.R., Wilson, J.D., 2014. High-throughout micro-late HCl-vanillin assay for screening tannin content in sorghum grain. J. Sci. Food Agric. 94, 2133–2136. https://doi.org/10.1002/jsfa.6538.

Iwatsuki, K., Boufford, D.E., Ohba, H., 2001. Flora of Japan IIb. Kodansha Ltd., Tokyo.

Jones, P., Messner, B., Nakajima, J., Schäffner, A.R., Saito, K., 2003. UGT73C6 and UGT78D1, glycosyltransferases involved in flavonol glycoside biosynthesis in *Arabidopsis thaliana*. J. Biol. Chem. 278, 43910–43918. https://doi.org/10.1074/jbc.M303523200.

Kaducová, M., Eliašová, A., Trush, K., Bačovčinová, M., Sklenková, K., Pal'ove-Balang, P., 2022. Accumulation of isoflavonoids in *Lotus corniculatus* after UV-B irradiation. Theor. Exp. Plant Physiol. 34, 53–62. https://doi.org/10.1007/s40626-021-00228-8.

Kaducová, M., Monje-Rueda, M.D., García-Calderón, M., Pérez-Delgado, C.M., Eliašová, A., Gajdošová, S., Petruľová, V., Betti, M., Márquez, A.J., Paľove-Balang, P., 2019. Induction of isoflavonoid biosynthesis in *Lotus japonicus* after UV-B irradiation. J. Plant Physiol. 236, 88–95. https://doi.org/10.1016/j.jplph.2019.03.003.

Kim, H.J., Kim, B.G., Ahn, J.H., 2013. Regioselective synthesis of flavonoid bisglycosides using *Escherichia coli* harboring two glycosyltransferases. Appl. Microbiol. Biotechnol. 97, 5275–5282. https://doi.org/10.1007/s00253-013-4844-7.

Kistner, C.N., Matamoros, M., 2005. RNA isolation using phase extraction and LiCl precipitation. In: Márquez, A.J. (Ed.), *Lotus Japonicus* Handbook. Springer, Dodrecht, pp. 123–124.

Krishnamurthy, P., Tsukamoto, C., Ishimoto, M., 2020. Reconstruction of the Evolutionary Histories of UGT Gene Superfamily in Legumes Clarifies the Functional Divergence of Duplicates in Specialized Metabolism. Int. J. Mol. Sci. 21, 1855 https://doi.org/10.3390/ijms21051855.

Kumar, S., Abedin, M.M., Singh, A.K., Das, S., 2020. Role of phenolic compounds in plant-defensive mechanisms. In: Lone, R., Shuab, R., Kamili, A. (Eds.), Plant Phenolics in Sustainable Agriculture. Springer, Singapore, pp. 517–532. https://doi.org/10.1007/978-981-15-4890-1_22.

Larbat, R., Olsen, K.M., Slimestad, R., Løvdal, T., Bénard, C., Verheul, M., Bourgaud, F., Robin, C., Lillo, C., 2012. Influence of repeated short-term nitrogen limitations on leaf phenolics metabolism in tomato. Phytochem 77, 119–128. https://doi.org/10.1016/j.phytochem.2012.02.004.

Lillo, C., Lea, U.S., Ruoff, P., 2008. Nutrient depletion as a key factor for manipulating gene expression and product formation in different branches of the flavonoid pathway. Plant Cell Environ. 31, 587–601. https://doi.org/10.1111/j.1365-3040.2007.01748.x.

Lim, E.K., Ashford, D.A., Hou, B., Jackson, R.G., Bowles, D.J., 2004. Arabidopsis glycosyltransferases as biocatalysts in fermentation for regioselective synthesis of diverse quercetin glucosides. Biotechnol. Bioeng. 87, 623–631. https://doi.org/10.1002/bit.20154.

Lotus Base, Genomic, proteomic & expression resources for *Lotus japonicus*. https://lotus.au.dk/(accessed 5 November 2022).

Márquez, A.J., Betti, M., García-Calderón, M., Pal'ove-Balang, P., Díaz, P., Monza, J., 2005. Nitrate assimilation in *Lotus japonicus*. J. Exp. Bot. 56, 1741–1749. https://doi.org/10.1093/jxb/eri171.

Myjakogusa.jp 3.0 Kazusa DNA Research Institute, http://www.kazusa.or.jp/lotus/index.html. (accessed 5 November 2022).

Modolo, L.V., Li, L., Pan, H., Blount, J.W., Dixon, R.A., Wang, X., 2009. Crystal structures of glycosyltransferase UGT78G1 reveal the molecular basis for glycosylation and deglycosylation of (iso)flavonoids. J. Mol. Biol. 392, 1292–1302. https://doi.org/10.1016/j.jmb.2009.08.017.

Mrázová, A., Belay, S.A., Eliašová, A., Perez-Delgado, C.M., Kaducová, M., Betti, M., Vega, J.M., Pal'ove-Balang, P., 2017. Expression, activity of phenylalanine-ammonia-lyase and accumulation of phenolic compounds in *Lotus japonicus* under salt stress. Biologia 72, 36–42. https://doi.org/10.1515/biolog-2017-0001.

Mun, T., Bachmann, A., Gupta, V., Stougaard, J., Andersen, S.U., 2016. *Lotus* base: an integrated information portal for the model legume *Lotus japonicus*. Sci. Rep. 6, 39447. https://doi.org/10.1038/srep39447.

Naoumkina, M.A., Zhao, Q., Gallego-Giraldo, L., Dai, X., Zhao, P.X., Dixon, R.A., 2010. Genome-wide analysis of phenylpropanoid defence pathways. Mol. Plant Pathol. 11, 829–846. https://doi.org/10.1111/j.1364-3703.2010.00648.x.

Neff, M.M., Chory, J., 1998. Genetic interactions between phytochrome A, phytochrome B, and cryptochrome during Arabidopsis development. Plant Physiol. 118, 27–36. https://doi.org/10.1104/pp.118.1.27.

Neugart, S., Bumke-Vogt, C., 2021. Flavonoid glycosides in *Brassica* species respond to UV-B depending on exposure time and adaptation time. Molecules 26, 494. https://doi.org/10.3390/molecules26020494.

Nezamivand-Chegini, M., Metzger, S., Moghadam, A., Tahmesebi, A., Koprivova, A., Eshghi, S., Mohammadi-Dehchesmeh, M., Kopriva, S., Niazi, A., Ebrahimie, E., 2022. Nitrogen and phosphorus deficiencies alter primary and secondary metabolites of soybean roots. bioRxiv 2022.03.14.484309. doi:10.1101/2022.03.14.484309.

Olsen, K.M., Slimestad, R., Lea, U.S., Brede, C., Løvdal, T., Ruoff, P., Verheul, M., Lillo, C., 2009. Temperature and nitrogen effects on regulators and products of the flavonoid pathway: experimental and kinetic model studies. Plant Cell Environ. 32, 286–299. https://doi.org/10.1111/j.1365-3040.2008.01920.x.

Prosser, I.M., Massonneau, A., Smyth, A.J., Waterhouse, R.N., Forde, B.G., Clarkson, D. T., 2006. Nitrate assimilation in the forage legume *Lotus japonicus* L. Planta 223, 821–834. https://doi.org/10.1007/s00425-005-0124-9.

Rambaut, A., Drummond, A.J., Xie, D., Baele, G., Suchard, M.A., 2018. Posterior summarisation in Bayesian phylogenetics using Tracer 1.7. Syst. Biol. 67, 901–904. https://doi.org/10.1093/sysbio/syy032.

Ren, G., Hou, J., Fang, Q., Sun, H., Liu, X., Zhang, L., Wang, P.G., 2012. Synthesis of flavonol 3-O-glycoside by UGT78D1. Glycoconj J. 29, 425–432. https://doi.org/10.1007/s10719-012-9410-5.

Rivai, R.R., Miyamoto, T., Awano, T., Takada, R., Tobimatsu, Y., Umezawa, T., Kobayashi, M., 2021. Nitrogen deficiency results in changes to cell wall composition of sorghum seedlings. Sci. Rep. 11, 23309. https://doi.org/10.1038/s41598-021-02570-y.

Rogato, A., D'Apuzzo, E., Barbulova, A., Omrane, S., Parlati, A., Carfagna, S., Costa, A., Lo Schiavo, F., Esposito, S., Chiurazzi, M., 2010. Characterization of a developmental root response caused by external ammonium supply in *Lotus japonicus*. Plant Physiol. 154, 784–795. https://doi.org/10.1104/pp.110.160309.

Ronquist, F., Teslenko, M., van der Mark, P., Ayres, D., Darling, A., Höhna, S., Larget, B., Liu, L., Suchard, M.A., Huelsenbeck, J.P., 2012. MrBayes 3.2: efficient Bayesian phylogenetic inference and model choice across a large model space. Syst. Biol. 61, 539–542.

Rubio-Wilhelmi, Mdel.M., Sanchez-Rodriguez, E., Leyva, R., Blasco, B., Romero, L., Blumwald, E., Ruiz, J.M., 2012. Response of carbon and nitrogen-rich metabolites to nitrogen deficiency in PSARK:IPT tobacco plants. Plant Physiol. Biochem. 57, 231–237. https://doi.org/10.1016/j.plaphy.2012.06.004.

Sánchez, L., Chaouiya, C., Thieffry, D., 2008. Segmenting the fly embryo: logical analysis of the role of the segment polarity cross-regulatory module. Int. J. Dev. Biol. 52, 1059–1075. https://doi.org/10.1387/ijdb.072439ls.

Suzuki, H., Sasaki, R., Ogata, Y., Nakamura, Y., Sakurai, N., Kitajima, M., Takayama, H., Kanaya, S., Aoki, K., Shibata, D., Saito, K., 2008. Metabolic profiling of flavonoids in *Lotus japonicus* using liquid chromatography Fourier transform ion cyclotron resonance mass spectrometry. Phytochemistry 69, 99–111. https://doi.org/10.1016/j.phytochem.2007.06.017.

Taguchi, G., Ubukata, T., Nozue, H., Kobayashi, Y., Takahi, M., Yamamoto, H., Hayashida, N., 2010. Malonylation is a key reaction in the metabolism of xenobiotic phenolic glucosides in Arabidopsis and tobacco. Plant J. 63, 1031–1041. https://doi.org/10.1111/j.1365-313X.2010.04298.x.

Tohge, T., Wendenburg, R., Ishihara, H., Nakabayashi, R., Watanabe, M., Sulpice, R., Hoefgen, R., Takayama, H., Saito, K., Stitt, M., Fernie, A.R., 2016. Characterization of a recently evolved flavonol-phenylacyltransferase gene provides signatures of natural light selection in *Brassicaceae*. Nat. Commun. 7, 12399. https://doi.org/10.1038/ncomms12399.

Tropper, M., Höhn, S., Wolf, L.S., Fritsch, J., Kastner-Detter, N., Rieck, C., Munkert, J., Meitinger, N., Lanig, H., Kreis, W., 2021. 21-Hydroxypregnane 21-O-malonylation, a crucial step in cardenolide biosynthesis, can be achieved by substrate-promiscuous BAHD-type phenolic glucoside malonyltransferases from *Arabidopsis thaliana* and homolog proteins from *Digitalis lanata*. Phytochemistry 187, 12710. https://doi.org/10.1016/j.phytochem.2021.112710.

Trush, K., Pal'ove-Balang, P., 2023. Accumulation and role of isoflavonoids in different environmental conditions. Plant Stress 8, 100153. https://doi.org/10.1016/j.stress.2023.100153.

Trush, K., Eliašová, A., Monje-Rueda, M.C., Kolarčík, V., Betti, M., Paľove-Balang, P., 2023. Chitosan is involved in elicitation of vestitol production in *Lotus japonicus*. Biol. Plant 67, 75–86. https://doi.org/10.32615/bp.2023.007.

Viskupicova, J., Strosova, M., Sturdik, E., Horakova, L., 2009. Modulating effect of flavonoids and their derivatives on sarcoplasmic reticulum Ca^{2+}-ATPase oxidized by hypochloric acid and peroxynitrite. Neuro. Endocrinol. Lett. 30 (Suppl. 1), 148–151.

Waki, T., Yoo, D., Fujino, N., Mameda, R., Denessiouk, K., Yamashita, S., Motohashi, R., Akashi, T., Aoki, T., Ayabe, S., Takahashi, S., Nakayama, T., 2016. Identification of protein-protein interactions of isoflavonoid biosynthetic enzymes with 2-hydroxyisoflavanone synthase in soybean (*Glycine max* (L.) Merr.). Biochem. Biophys. Res. Commun. 469, 546–551. https://doi.org/10.1016/j.bbrc.2015.12.038.

Wellburn, A.R., 1994. The spectral determination of chlorophylls a and b, as well as total carotenoids, using various solvents with spectrophotometers of different resolution. J. Plant. Physiol. 144, 307–313. https://doi.org/10.1016/S0176-1617(11)81192-2.

Wen, Z., Kaiser, B.N., 2018. Unraveling the functional role of NPF6 transporters. Front. Plant Sci. 9, 973. https://doi.org/10.3389/fpls.2018.00973.

Yin, Q., Shen, G., Chang, Z., Tang, Y., Gao, H., Pang, Y., 2017. Involvement of three putative glucosyltransferases from the UGT72 family in flavonol glucoside/rhamnoside biosynthesis in *Lotus japonicus* seeds. J. Exp. Bot. 68, 597–612. https://doi.org/10.1093/jxb/erw420.

Yonekura-Sakakibara, K., Tohge, T., Matsuda, F., Nakabayashi, R., Takayama, H., Niida, R., Watanabe-Takahashi, A., Inoue, E., Saito, K., 2008. Comprehensive flavonol profiling and transcriptome coexpression analysis leading to decoding gene-metabolite correlations in *Arabidopsis*. Plant Cell 20, 2160–2176. https://doi.org/10.1105/tpc.108.058040.

Tamura, K., Stecher, G., Kumar, S., 2021. MEGA11: molecular evolutionary genetics analysis version 11. Mol. Biol. Evol. 38, 3022–3027. https://doi.org/10.1093/molbev/msab120.

Yu, X.H., Chen, M.H., Liu, C.J., 2008. Nucleocytoplasmic-localized acyltransferases catalyze the malonylation of 7-O-glycosidic (iso)flavones in *Medicago truncatula*. Plant J. 55, 382–396. https://doi.org/10.1111/j.0960-7412.2008.03509.x.

Zavala, J.A., Mazza, C.A., Dillon, F.M., Chludil, H.D., Ballaré, C.L., 2015. Soybean resistance to stink bugs (*Nezara viridula* and *Piezodorus guildinii*) increases with exposure to solar UV-B radiation and correlates with isoflavonoid content in pods under field conditions. Plant, Cell Environ. 38, 920–928. https://doi.org/10.1111/pce.12368.

Zhang, W., Wu, L., Ding, Y., Yao, X., Wu, X., Weng, F., Li, G., Liu, Z., Tang, S., Ding, C., Wang, S., 2017. Nitrogen fertilizer application affects lodging resistance by altering secondary cell wall synthesis in japonica rice (*Oryza sativa*). J. Plant Res. 130, 859–871. https://doi.org/10.1007/s10265-017-0943-3.

Zhang, X., Liu, C.J., 2015. Multifaceted regulations of gateway enzyme phenylalanine ammonia-lyase in the biosynthesis of phenylpropanoids. Mol. Plant 8, 17–27. https://doi.org/10.1093/mp/ssu134.